# Critical Terrace Width for Two-Dimensional Nucleation during Si Growth on Si(111)-(7 × 7) Surface

D. I. Rogilo,[1,2,*] L. I. Fedina,[1] S. S. Kosolobov,[1,2] B. S. Ranguelov,[3] and A. V. Latyshev[1,2]

[1]*Institute of Semiconductor Physics SB RAS, Academician Lavrentiev Avenue 13, Novosibirsk 630090, Russia*

[2]*Novosibirsk State University, Pirogov Street 2, Novosibirsk 630090, Russia*

[3]*Institute of Physical Chemistry BAS, Academician Georgi Bonchev Street, Building 11, Sofia 1113, Bulgaria*

(Received 24 September 2012; revised manuscript received 30 May 2013; published 19 July 2013)

The critical terrace width $\lambda$ for 2D island nucleation and growth (2DNG) on large-scale atomically flat terraces of a step-bunched Si(111)-(7 × 7) surface has been studied by *in situ* ultrahigh vacuum reflection electron microscopy as a function of the substrate temperature $T$ and Si deposition rate $R$. The dependence of $\lambda^2(R)$ is characterized by a power law with scaling exponent $\chi = 1.36$–$1.46$, validating an attachment limited (AL) growth kinetics up to 720 °C. At this temperature, the Arrhenius dependencies $\ln\lambda^2(1/T)$ change their slope, so that the effective 2DNG activation energy $E_{2D}$ drops from 2.4 eV down to 0.5 eV at $T > 720$ °C. We first show that the $E_{2D}$ change is caused by a transition between AL and DL (diffusion limited) growth kinetics accompanied by a step shape transformation. The AL growth mode is characterized by kinetic length $d_- \sim 10^5 a$ and the preferential step-down attachment of atoms to steps limited by an energy barrier $E_{ES}^- \approx 0.9$ eV.

DOI: 10.1103/PhysRevLett.111.036105 PACS numbers: 68.55.ag, 68.47.Fg, 81.16.Rf

The control of atomic processes on crystal surfaces during epitaxial growth is the basis of contemporary and future solid-state nanotechnology. The atomic scale design of the surface morphology only becomes possible with a profound understanding of the surface instabilities induced during surface treatments and epitaxial growth, both leading to a surface roughening (e.g., step bunching, meandering, and mound formation). Various theoretical models have been developed to analyze this surface roughening and to account for a great number of atomic processes affecting surface instabilities (see Ref. [1] for a review). These phenomena obey scaling relations defined by atomic mechanisms. However, the scaling exponents have been shown to depend only on a single parameter (a universality class), which could be attributed to different mechanisms [2]. Therefore, despite its convenience, this formalism does not provide the exact microscopic mechanism for surface instability under certain conditions and does not explain the transitions between universality classes.

To obtain detailed information about the atomic processes on crystal surface, a number of experimental techniques have been used [3–13]. They allow analyzing the atomic step distribution [3,4], 2D island size distribution [5,6], and island concentration $N_{2D}$ [6–9] as functions of substrate temperature $T$ and the deposition rate $R$. However, in spite of extensive research, the mechanisms of the surface mass transport on a Si(111) surface, including the diffusion of atoms on the terraces and across steps as well as the attachment of atoms at step edges, are still controversial [10–13]. The authors of Ref. [10] provide evidence of significant mass transport across the atomic steps, suggesting that the steps are highly permeable at $T = 450$–$550$ °C while the opposite is proven at $T = 530$ °C in Ref. [11]. It is also stated that 2D island decay is governed by atom attachment or detachment at the step edges [attachment limited (AL) kinetics] [12], but diffusion limited mode (DL kinetics) is found under similar conditions in Ref. [13]. Furthermore, the problem becomes more complex due to the absence of experimentally determined values of some key parameters: the energy barriers for adatom attachment at the steps and the kinetic length $d_\pm$. The evaluation of $d_\pm$ is particularly important since it defines whether the DL ($d_\pm \ll l$) or the AL ($d_\pm \gg l$) kinetic mode is realized [11]:

$$d_\pm = D/K_\pm = a(\nu_{dif}/\nu_\pm)\exp(E_{ES}^\pm/kT). \quad (1)$$

Here, $l$ is the interstep distance, $D$ is the surface diffusion constant [$a = 0.384$ nm for the Si(111) surface], $k$ is Boltzmann's constant, $K_+$ ($K_-$) is the kinetic coefficient for adatom attachment to an ascending (descending) step, and $\nu_{dif}$, $\nu_+$, and $\nu_-$ are the attempt frequencies for, respectively, the diffusive motion on a terrace, at a lower step edge, and at an upper step edge. $E_{ES}^+$ and $E_{ES}^-$ are Ehrlich–Schwöbel (ES) and inverse ES energy barriers for atom attachment to an ascending and to a descending step, respectively. These barriers are in addition to the surface diffusion activation energy $E_d$, but only the smallest one of them limits the growth kinetics in the AL mode [14]. The parameters $K_\pm$, $d_\pm$, and the step permeability have been theoretically shown to be related to the step kink density [15].

In this Letter, we first show that the AL ⇒ DL kinetic transition during Si growth on a Si(111)-(7 × 7) surface takes place at $T$ around 720 °C. This transition is accompanied by a step shape transformation from zigzag to smooth, and leads to a drop in the activation energy from

 

2.4 to 0.5 eV. We have found that AL Si growth is limited by preferential atom attachment to descending steps, with an energy barrier $E_{ES}^{-} \sim 0.9$ eV.

The classical treatment of crystal growth implies that the growth of a 2D island starts with the formation of a stable nucleus consisting of more than $i$ atoms. It occurs when the distance between the atomic steps exceeds a critical terrace width $\lambda$. This approach implies that adatom attachment to a step takes place without an energy barrier: the growth kinetics is therefore limited only by surface diffusion. In this case, the dependence $\lambda(T, R)$ turns into a classical law [9]:

$$\lambda^2 \propto N_{2D}^{-1} \propto R^{-\chi} \exp(-E_{2D}/kT), \quad (2)$$

where $N_{2D}$ is the maximum concentration of stable clusters and 2D islands, $\chi$ is the scaling exponent, and $E_{2D}$ is the effective 2D island nucleation and growth (2DNG) activation energy.

When the energy barrier for atom attachment to a step is significant, the equation for $\lambda(T, R)$ remains the same, but $E_{2D}^{DL} \neq E_{2D}^{AL}$, and the expressions for the parameter $\chi$ are different [16]:

$$\chi^{DL} = i/(i+2), \quad (3)$$

$$\chi^{AL} = 2i/(i+3), \quad (4)$$

where $i$ is the critical nucleus size; the subscript DL or AL possessed by $E_{2D}$ and $\chi$ indicates which growth kinetics is obtained: under DL conditions, the parameter $\chi^{DL}$ is always less than unity for every integer $i \geq 0$ [Eq. (3)]. If AL is obtained, the parameter $\chi^{AL}$ is allowed to be greater than unity [Eq. (4)]. When Eq. (4) was derived [16], it provided the explanation for the experimental observations of $\chi > 1$ [17]. However, a unified analytical expression $\lambda(T, R)$ accounting for the transition between DL and AL kinetics has not been derived until recently [14]. We used this general approach to analyze our experimental dependencies $\lambda(T, R)$.

*In situ* experiments were carried out in an ultrahigh vacuum reflection electron microscope (UHV REM) equipped with a silicon evaporator. We used specimens with dimensions $8 \times 1.1 \times 0.3$ mm$^3$ cut from $n$-type (0.3 $\Omega \cdot$ cm) Si(111) wafers with the miscut angle less than 1 deg. The details of the UHV REM technique and sample preparation were described elsewhere [18]. The samples were cleaned in the UHV chamber at $T \approx 1300$ °C by passing alternating current through the sample: during this treatment, a regular distribution of monatomic steps was formed [Fig. 1(a)]. The important feature of the REM technique is that the images are compressed by about 50 times along the beam incidence. This contraction leads to the wavy contrast from the smooth and almost parallel to the beam direction atomic steps in the REM images [see Fig. 1(a)]. After the cleaning procedure, the large-scale (up to 20 $\mu$m in width, $W_{in}$) atomically flat terraces

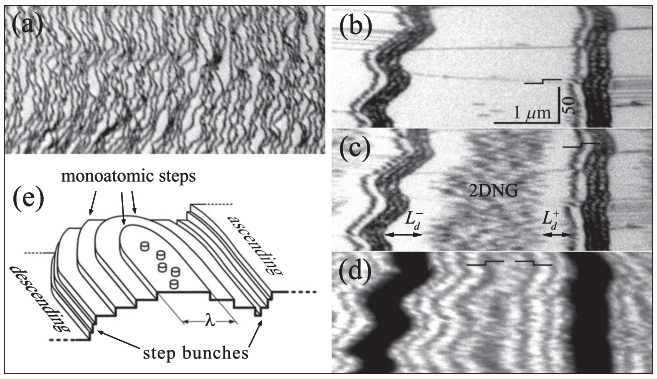


FIG. 1. REM images of (a) an initial atomically clean Si(111) surface, (b) a large-scale atomically flat terrace between two step bunches, (c) the same terrace with 0.12 ML of Si deposited at 600 °C, and (d) a pyramidlike structure after prolonged Si deposition. (e) Schematic representation of pyramidlike pattern.

separated by step bunches (i.e., groups of closely placed monatomic steps) were induced on the sample surface during dc heating at $T = 1100$–$1270$ °C [19]. Figure 1(b) shows a REM image of such a terrace bounded by a descending step bunch at the left and by an ascending step bunch at the right. The step bunches appear in the REM images as pronounced wavy black stripes, and the terraces as bright areas. After slow sample cooling to $T < 830$ °C, a $(1 \times 1) \Rightarrow (7 \times 7)$ phase transition takes place on the Si(111) surface [20], preserving the existing large-scale terraces. Since the initial terrace width $W_{in}$ is sufficiently greater than a certain critical width $\lambda$, we observe clear nucleation of 2D islands when the Si deposition starts [Fig. 1(c)]. At the same time, near the step bunches, which serve as effective sinks for adatoms, large denuded zones appear. One can see that the denuded zone $L_d^-$ near the descending step bunch is about 30% wider than the $L_d^+$ near the ascending step bunch, which authenticates the preferential adatom sink to descending steps. After the deposition of from tens to hundreds Si monolayers (ML) (1 ML $= 1.56 \times 10^{15}$ cm$^{-2}$), the width of the uppermost layer is reduced to $\lambda$, and a steady-state growth of the pyramidlike structure is established [Figs. 1(d) and 1(e)].

The time evolution of this pattern is periodic at fixed $T$ and $R$, and it is repeated after each Si monolayer is deposited. During the period, all layers of the pyramidlike pattern widen, owing to a step flow caused by adatom attachment. At the same time, there is no observable displacement of the step bunches, due to the large number of steps they contain. When the width of the uppermost layer reaches a critical value $\lambda$, the nucleation of new 2D islands occurs on top of this layer. The growth of these islands is followed by their coalescence (2DNG), which leads to the formation of a new 2D layer. Then the process is repeated.

A REM image of the pyramidlike structure formed at $T = 600$ °C and $R = 10^{-2}$ ML/s is shown in Fig. 1(d). One can see that the width of the REM contrast from the

monatomic steps increases up to 10 times during the growth, as compared to the REM step contrast at the initial surface [Fig. 1(a)], which suggests a significant modification of the step shape. We used, therefore, *ex situ* atomic force microscopy (AFM) to investigate the step shape and surface morphology in more detail.

Figures 2(a) and 2(b) show topographical AFM images of the pyramidlike patterns formed on the Si(111)-(7 × 7) surface after durational Si growth at 650 °C and 750 °C, respectively. In both cases, 2D islands nucleate on top of many stacked 2D layers [Fig. 2(a)]. However, at the lower temperature, the islands have a clear triangular faceting of the edges aligned along the ⟨110⟩ directions. The coalescence of such islands followed by step-flow growth leads to the formation of zigzag monatomic steps. This explains why the REM image of the steps becomes much wider and fuzzier during low-$T$ Si growth [Fig. 1(d)]. At the same time, the pyramidlike pattern formed at 750 °C at a very large (up to 20 $\mu$m) atomically flat terrace displays a concentration of 2D islands which is less by about 2 orders of magnitude, permitting the growth of separate pyramids. In this case, we observe much smoother meandering steps, which corresponds to a much higher density of kinks at the step edges [Fig. 2(b)].

It is known that the formation and propagation of step kinks on a Si(111)-(7 × 7) surface have specific microscopic features related to the surface reconstruction and the existence of the stacking fault in a half-unit cell (HUC) [5]. Thus, both processes become dependent on the mutual orientation of the step edge and the faulted HUC. According to *in situ* STM study, the growth of a single triangular 2D island is limited by the nucleation of a new faulted HUC at the straight $[\bar{1}\,\bar{1}\,2]$-type island edge accompanied by the lift of the underlying stacking fault [5]. One can regard this new HUC as a double kink at the straight island edge. In fact, the (7 × 7) reconstructed surface looks like a patchy Shockley dislocation whose climbing during step propagation is limited by the double kink nucleation at the $[\bar{1}\,\bar{1}\,2]$-type step edge (in this analogy, the double kink is the jog of the Shockley dislocation). The double kink nucleation is much less frequent than the subsequent attachment of atoms to both sides of the double kink, which causes rapid propagation of kinks towards the island corners and leads to a step alignment with $[\bar{1}\,\bar{1}\,2]$-type directions. The rare double kink nucleation therefore limits atom attachment at straight steps and may cause AL growth kinetics, the triangular shape of the 2D islands, and the zigzag shape of the monatomic steps [Fig. 2(a)].

Figure 3(a) shows the experimental dependencies $\lambda^2(R)$ at fixed $T$ with slopes equal to the scaling exponents $\chi$ [Eq. (2)]. One can see that the plots obtained at high $R$ and/or large $W_{\text{in}}$ are characterized by values $\chi = 1.36$–$1.46$, indicating AL kinetics up to $T = 720$ °C [Eq. (4)]. The greater $T$ is, the higher $R$ is necessary to observe AL kinetics. Note that the $\chi$ decreases when $W_{\text{in}} < 2$ $\mu$m and $R < 0.08$ ML/s at $T = 650$ °C (compare plots filled circle and open circle). We attribute this change to the impact of step permeability on $\lambda$. The discussion of this effect is beyond the scope of this Letter, but it could be neglected at large $W_{\text{in}}$ and high $R$. The AL kinetics has also been reported in *ex situ* AFM study of unstable step-flow Si growth on vicinal Si(111)-(7 × 7) surface miscut 1°–5.6° to the $[\bar{1}\,\bar{1}\,2]$ direction [21]. The scaling properties of zigzag step bunches with straight $[\bar{1}\,\bar{1}\,2]$-type step edges have been shown to be consistent with AL kinetics at $T = 600$ °C–775 °C. When treating the microscopic features of the kinks at the $[\bar{1}\,\bar{1}\,2]$-type step edges mentioned above, one can conclude that the double kink nucleation limits the AL growth in our experiments and in both Refs. [5,21].

Figure 3(b) displays the experimental dependencies $\lambda^2(1000/T)$ plotted in Arrhenius coordinates at fixed $R \geq 0.08$ ML/s. The slope of each plot ($E_{2D}$) changes at $T$ around 720 °C. In particular, the exponential fitting of the plot of $\lambda^2(1000/T, R = 0.135$ ML/s) gives $E_{2D} \approx 2.4$ eV within the range $T = 620$ °C–720 °C. This value is close to 2.0 and 2.2 eV obtained at $T < 600$ °C in Refs. [22,23], respectively. However, we have found that $E_{2D}$ drops to 0.5 eV at $T > 720$ °C. This sharp change in $E_{2D}$ is accompanied by a significant modification of the step shape: from the zigzag one of Fig. 2(a) to the smooth one of Fig. 2(b). The increase in the kink density at smooth steps strongly facilitates atom solidification at the step edges, which, in turn, triggers the transition from the AL

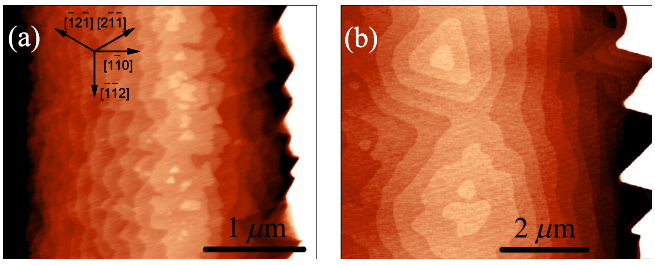


FIG. 2 (color online). Topographical AFM images of Si(111) surface with a pyramidlike pattern created at (a) 650 °C and (b) 750 °C.

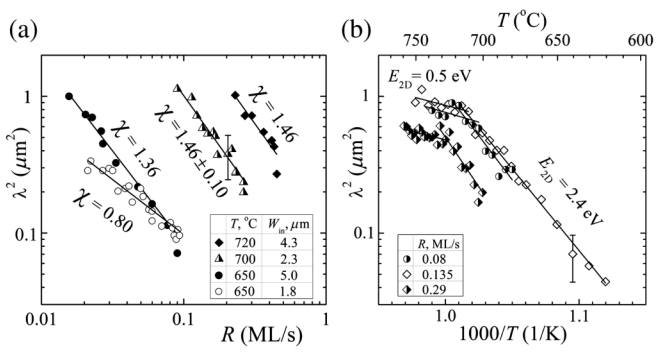


FIG. 3. Experimental dependence of $\lambda^2$ on (a) deposition rate $R$ and (b) substrate temperature $T$. The typical error bars are given for two experimental plots.

growth kinetic mode to the DL one. We can thus establish a link between the step shape modification, the $E_{2D}$ jump, and the AL $\Leftrightarrow$ DL kinetic transition.

We analyzed the obtained $\chi$ and $E_{2D}$ within the scope of the theoretical approach developed in Ref. [14]. The expression $\lambda(T, R)$ derived there accounts for both cases of DL and AL regimes as high-$T$ and low-$T$ limits, respectively, where the expression turns into Eq. (2) with different equations for $E_{2D}$ and $\chi$ [Eqs. (3) and (4)]. The dependence $\ln\lambda^2(1/T)$ derived at constant $R$ therefore undergoes a change in $E_{2D}$ caused by the transition in kinetics AL $\Leftrightarrow$ DL. This approach also accounts for the step permeability and asymmetrical ES barriers $E_{ES}^{\pm}$. The step permeability has been shown to affect only the transition region between these two regimes, the extreme values $E_{2D}^{DL}$ and $E_{2D}^{AL}$ being independent of the step permeability in the high-$T$ and low-$T$ limits, respectively:

$$E_{2D}^{DL} = \frac{E_i + iE_d}{i+2}, \tag{5}$$

$$E_{2D}^{AL} = 2\frac{E_i + iE_d + (i+1)E_{ES}}{i+3}, \tag{6}$$

where $E_{ES} = \min\{E_{ES}^{+}, E_{ES}^{-}\}$, and $E_i$ is the energy gain after the formation of a critical nucleus from $i$ adatoms (critical nucleus binding energy).

Since we have observed the favored sink of adatoms to descending steps of the bunch [see Fig. 1(c)], we conclude that the inverse ES barrier $E_{ES}^{-}$ is less than $E_{ES}^{+}$, and $E_{ES}^{-}$ thus governs the AL $\Leftrightarrow$ DL transition we have found. Using Eqs. (5) and (6), one can obtain

$$E_{ES}^{-} = E_{ES} = \frac{i+3}{2(i+1)}E_{2D}^{AL} - \frac{i+2}{i+1}E_{2D}^{DL}. \tag{7}$$

We have obtained the fitting $\chi = 1.46 \pm 0.10$ at $T = 700\,^{\circ}\mathrm{C}$ [Fig. 3(a)] that corresponds to the critical nucleus consisting of 7–10 atoms [Eq. (4)]. Using the mean value, $i = 8$ [$\chi_{i=8} \approx 1.455$ from Eq. (4)], and the best fitting activation energies, $E_{2D}^{DL} = 0.5$ eV and $E_{2D}^{AL} = 2.4$ eV [Fig. 3(b)], one finds from Eq. (7) that $E_{ES}^{-} \approx 0.9$ eV. When assuming $\nu_{dif} \sim \nu_{edge}$ in Eq. (1), one can obtain $d_{-} \sim 10^5 a$, which corresponds to clear AL kinetics [24]. To be specific, for the reasons discussed above, it is limited by double kink nucleation at the straight $[\bar{1}\,\bar{1}\,2]$-type step edge, and the energy barrier $E_{ES}^{-} \approx 0.9$ eV is associated with this process. However, the kink density at $T \gtrsim 720\,^{\circ}\mathrm{C}$ becomes so large that atom solidification at the step edges is strongly facilitated, and the growth mode switches to DL kinetics.

In conclusion, we have studied in detail the dependence of the critical terrace width $\lambda(T, R)$ for 2D island nucleation on a Si(111)-(7 × 7) surface by *in situ* UHV REM. The clear AL growth mode takes place at large-scale terraces and at high deposition rates. Our results elucidate the mechanism of the AL $\Leftrightarrow$ DL kinetic transition observed around 720 °C: it is governed by the favored step-down atom attachment limited by the energy barrier $E_{ES}^{-} \approx 0.9$ eV that impedes double kink nucleation at the straight $[\bar{1}\,\bar{1}\,2]$-type step edge.

The authors would like to thank Professor S. Stoyanov for his helpful discussions. This work was performed on the basis of the Center of Cooperative Use and was partially supported by programs of the Ministry of Education and Science of the Russian Federation (Contract No. 16.552.11.7091). B. S. R. is grateful for the financial help of Project BG051PO001-3.3.06-0038.

*rogilo@isp.nsc.ru

[1] C. Misbah, O. Pierre-Louis, and Y. Saito, Rev. Mod. Phys. **82**, 981 (2010).
[2] A. Pimpinelli, V. Tonchev, A. Videcoq, and M. Vladimirova, Phys. Rev. Lett. **88**, 206103 (2002).
[3] T. Frisch and A. Verga, Phys. Rev. Lett. **96**, 166104 (2006).
[4] H.-C. Jeong and E. D. Williams, Surf. Sci. Rep. **34**, 171 (1999).
[5] B. Voigtländer, M. Kästner, and P. Šmilauer, Phys. Rev. Lett. **81**, 858 (1998).
[6] Y. A. Kryukov and J. G. Amar, Phys. Rev. B **81**, 165435 (2010).
[7] V. Cherepanov and B. Voigtländer, Phys. Rev. B **69**, 125331 (2004).
[8] S. Filimonov, V. Cherepanov, Y. Hervieu, and B. Voigtländer, Phys. Rev. B **76**, 035428 (2007).
[9] J. A. Venables, Surf. Sci. **299–300**, 798 (1994).
[10] U. Köhler, J. E. Demuth, and R. J. Hamers, J. Vac. Sci. Technol. A **7**, 2860 (1989).
[11] W. F. Chung and M. S. Altman, Phys. Rev. B **66**, 075338 (2002).
[12] A. Ichimiya, K. Hayashi, E. D. Williams, T. L. Einstein, M. Uwaha, and K. Watanabe, Phys. Rev. Lett. **84**, 3662 (2000).
[13] S. Hildebrandt, A. Kraus, R. Kulla, G. Wilhelmi, M. Hanbücken, and H. Neddermeyer, Surf. Sci. **486**, 24 (2001).
[14] B. Ranguelov, M. S. Altman, and I. Markov, Phys. Rev. B **75**, 245419 (2007).
[15] M. Sato, Eur. Phys. J. B **59**, 311 (2007).
[16] D. Kandel, Phys. Rev. Lett. **78**, 499 (1997).
[17] I.-S. Hwang, T.-C. Chang, and T. T. Tsong, Phys. Rev. Lett. **80**, 4229 (1998).
[18] A. V. Latyshev, A. B. Krasilnikov, and A. L. Aseev, Phys. Rev. B **54**, 2586 (1996).
[19] A. Latyshev, A. Aseev, A. Krasilnikov, and S. Stenin, Surf. Sci. **213**, 157 (1989).
[20] K. Takayanagi, Y. Tanishiro, M. Takahashi, and S. Takahashi, J. Vac. Sci. Technol. A **3**, 1502 (1985).
[21] H. Omi, Y. Homma, V. Tonchev, and A. Pimpinelli, Phys. Rev. Lett. **95**, 216101 (2005).
[22] A. Fissel, M. Oehme, K. Pfennighaus, and W. Richter, Surf. Sci. **383**, 370 (1997).
[23] W. F. Chung, K. Bromann, and M. S. Altman, Int. J. Mod. Phys. B **16**, 4353 (2002).
[24] K. Man, A. Pang, and M. Altman, Surf. Sci. **601**, 4669 (2007).